0026-895X/07/7201-182–190$20.00
MOLECULAR PHARMACOLOGY
Copyright © 2007 The American Society for Pharmacology and Experimental Therapeutics
Mol Pharmacol 72:182–190, 2007

Vol. 72, No. 1
33670/3222840
Printed in U.S.A.

Activation of the Angiotensin II Type 1 Receptor Leads to Movement of the Sixth Transmembrane Domain: Analysis by the Substituted Cysteine Accessibility Method

Stéphane S. Martin, Brian J. Holleran, Emanuel Escher, Gaétan Guillemette, and Richard Leduc

Department of Pharmacology, Faculty of Medicine and Health Sciences, Université de Sherbrooke, Sherbrooke, Quebec, Canada

Received December 20, 2006; accepted April 18, 2007

ABSTRACT

The role of transmembrane domain six (TMD6) of the angiotensin II type 1 receptor, which is predicted to undergo conformational changes after agonist binding, was investigated using the substituted-cysteine accessibility method. Each residue in the Lys240–Leu265 fragment was mutated, one at a time, to a cysteine. The resulting mutants were expressed in COS-7 cells, which were subsequently treated with the charged sulfhydryl-specific alkylating agent methanethiosulfonate-ethylammonium (MTSEA). This treatment led to a significant reduction in binding of ^{125}I-[Sar^1,Ile^8]AngII to the F249C, H256C, T260C, and V264C mutant receptors, suggesting that these residues orient themselves within the water-accessible binding pocket of the AT_1 receptor. It is noteworthy that this pattern of acquired MTSEA sensitivity was altered for TMD6 cysteines engineered in a constitutively active AT_1 receptor. Indeed, mutant F249C was insensitive to MTSEA treatment, whereas the sensitivity of mutant V264C decreased. Under these conditions, one other mutant, F261C, was found to be sensitive to MTSEA treatment. Our results suggest that constitutive activation of the AT_1 receptor causes TMD6 to pivot. This movement moves the top (extracellular side) of TMD6 toward the binding pocket and simultaneously distances the bottom (intracellular side) away from the binding pocket. Using this approach, we identified key elements within TMD6 that contribute to the activation of class A GPCRs through structural rearrangements.

The octapeptide hormone angiotensin II (AngII) is the active component of the renin-angiotensin system. It exerts a wide variety of physiological effects, including vascular contraction, aldosterone secretion, neuronal activation, and cardiovascular cell growth and proliferation (de Gasparo et al., 2000). Many of the known physiological effects of AngII are produced through the activation of the AT_1 receptor, which belongs to the G protein-coupled receptor superfamily (Burnier, 2001; Miura et al., 2003).

Like other GPCRs, the AT_1 receptor undergoes spontaneous isomerization between its inactive state (favored in the absence of agonist) and its active state (induced or stabilized by the agonist) (Gether and Kobilka, 1998). Movement of TMD helices through translational or rotational displacement is believed to be essential to achieve the active state (Dunham and Farrens, 1999; Rasmussen et al., 1999; Ghanouni et al., 2001). For the AT_1 receptor, it has been proposed that TMD3, TMD5, TMD6, and TMD7 participate in the activation process by providing a network of interactions through the AngII-binding pocket (Inoue et al., 1997). The dynamics of this network are thought to be modified by agonist binding, which forces the receptor to either form or abolish interactions within the TMDs.

The substituted-cysteine accessibility method (SCAM) (Akabas et al., 1992; Javitch et al., 1994, 2002) is an ingenious approach for systematically identifying residues in a TMD that contribute to the binding-site pocket of a G protein-coupled receptor. Consecutive residues within TMDs are mutated to cysteine, one at a time, and the mutant receptors are expressed in heterologous cells. If ligand binding to a cysteine-substituted mutant is unchanged compared with

This work was supported by the Canadian Institutes of Health Research and is part of the M.Sc. thesis of S.S.M. R.L. is a Chercheur National of the Fonds de la Recherche en Santé du Québec. E.E. is recipient of the J.C. Edwards Chair in Cardiovascular Research. S.S.M. is the recipient of a studentship from the Heart and Stroke Foundation of Canada.

Article, publication date, and citation information can be found at http://molpharm.aspetjournals.org.

doi:10.1124/mol.106.033670.

ABBREVIATIONS: AngII, angiotensin II; AT_1 receptor, angiotensin II type-1 receptor; TMD, transmembrane domain; SCAM, substituted-cysteine accessibility method; MTSEA, methanethiosulfonate-ethylammonium; PCR, polymerase chain reaction; DMEM, Dulbecco's modified Eagle's medium; PBS, phosphate-buffered saline; MPA, methionine proximity assay; IP, inositol phosphate.

the wild-type receptor, it is assumed that the structure of the mutant receptor, especially around the binding site, is similar to that of wild-type and therefore that the substituted cysteine lies in an orientation similar to that of the wild-type residue. In TMDs, the sulfhydryl of a cysteine oriented toward the binding-site pocket should react more quickly with a positively charged sulfhydryl reagent such as methanethiosulfonate-ethylammonium (MTSEA) than sulfhydryls facing the interior of the protein or the lipid bilayer.

Two criteria are used to determine whether engineered cysteines are positioned at the surface of the binding-site pocket: 1) the reaction with MTSEA alters binding irreversibly and 2) the reaction is retarded by the presence of ligand. We previously used this approach to identify residues in TMD7 and TMD3 that line the surface of the binding-site pocket in the wild-type AT_1 receptor and in the constitutively active N111G-AT_1 receptor (Boucard et al., 2003; Martin et al., 2004). It had been demonstrated that substitution of Asn111 for a residue of smaller size (Ala or Gly) confers constitutive activity on the AT_1 receptor, thereby establishing a reliable model of a receptor in an active state (Balmforth et al., 1997; Groblewski et al., 1997; Feng et al., 1998). Here, we report the application of SCAM to probe TMD6 in the wild-type receptor and in a constitutively active AT_1 receptor.

Materials and Methods

Materials. Bovine serum albumin, bacitracin, and soybean trypsin inhibitor were from Sigma Chemical Co. (St. Louis, MO). The sulfhydryl-specific alkylating reagent MTSEA (CH_3SO_2-$SCH_2CH_2NH_3^+$) was from Toronto Research Chemicals, Inc. (Toronto, ON, Canada). The cDNA clone for the human AT_1 receptor subcloned in the mammalian expression vector pcDNA3 was kindly provided by Dr. Sylvain Meloche (Université de Montréal, Montréal, QC, Canada). LipofectAmine2000 and culture media were from Invitrogen (Carlsbad, CA). ^{125}I-[Sar^1,Ile^8]AngII (specific radioactivity, ~1500 Ci/mmol) was prepared using Iodo-GEN (Perbio Science, Erembodegem, Belgium) according to the method of Fraker and Speck (1978) and as reported previously (Guillemette and Escher, 1983).

Numbering of Residues in TMD6. Residues in TMD6 of the human AT_1 receptor were given two numbering schemes. First, residues were numbered according to their positions in the human AT_1 receptor sequence. Second, residues were also indexed according to their positions relative to the most conserved residue in the TMD in which they are located (Ballesteros and Weinstein, 1995). By definition, the most conserved residue was assigned index position "50." For example, in TMD6, Pro255 is the most conserved residue and was designated Pro255$^{(6.50)}$; Ile254$^{(6.49)}$ and His256$^{(6.51)}$ are the adjacent N- and C-terminal residues, respectively, of Pro255$^{(6.50)}$. This indexing scheme simplifies the identification of aligned residues in different GPCRs of the same class.

Oligodeoxynucleotide Site-Directed Mutagenesis. Site-directed mutagenesis was performed on the wild-type AT_1 receptor using the overlap PCR method (Expand High-Fidelity PCR System; Roche Diagnostics, Laval, QC, Canada). In brief, forward and reverse oligonucleotides were constructed to introduce cysteine mutations between Lys240$^{(6.35)}$ and Leu265$^{(6.60)}$. PCR products were subcloned into the HindIII-XbaI sites of the mammalian expression vector pcDNA3.1. Site-directed mutations were then confirmed by automated DNA sequencing by aligning the AT_1 sequence with multiAlin (Corpet, 1988).

Cell Culture and Transfections. COS-7 cells were grown in Dulbecco's modified Eagle's medium (DMEM) containing 2 mM L-glutamine and 10% (v/v) fetal bovine serum. The cells were seeded into 100-mm culture dishes at a density of 2×10^6 cells/dish. When cells were at ~90% confluence, they were transfected with 4 μg of plasmid DNA and 15 μl of LipofectAmine2000. After 24 h, transfected cells were trypsinized, distributed into 12-well plates, and grown for an additional 24 h in complete DMEM containing 100 IU/ml penicillin and 100 μg/ml streptomycin before MTSEA treatment and binding assay were performed.

Binding Experiments COS-7 cells were grown for 36 h after transfection in 100-mm culture dishes, washed once with phosphate-buffered saline (PBS), and subjected to one freeze-thaw cycle. Broken cells were then gently scraped into washing buffer (25 mM Tris-HCl, pH 7.4, 100 mM NaCl, 5 mM $MgCl_2$), centrifuged at 2500 *g* for 15 min at 4°C, and resuspended in binding buffer (25 mM Tris-HCl, pH 7.4, 100 mM NaCl, 5 mM $MgCl_2$, 0.1% BSA, 0.01% bacitracin, 0.01% soybean trypsin inhibitor). Saturation binding experiments were done by incubating broken cells (20–40 μg of protein) for 1 h at room temperature with increasing concentrations of ^{125}I-[Sar^1,Ile^8]AngII in a final volume of 500 μl. Nonspecific binding was determined in the presence of 1 μM unlabeled [Sar^1,Ile^8]AngII. Bound radioactivity was separated from free ligand by filtration through GF/C filters presoaked for at least 3 h in binding buffer. Receptor-bound radioactivity was evaluated by γ counting.

Intracellular IP Accumulation Measurement. Inositol phosphate accumulation was determined as described previously (Lanctôt et al., 1999). In brief, basal production of inositol phosphates was measured after this modification: COS-7 cells were seeded in six-well plates, transfected, and labeled for 16 h in serum-free, inositol free M199 containing 10 μCi/ml [*myo*-^{3}H]inositol (GE Healthcare, Chalfont St. Giles, Buckinghamshire, UK). Cells were washed twice with PBS/0.1%(w/v) dextrose and then incubated in stimulation buffer (DMEM containing 25 mM HEPES, 10 mM LiCl, and 0.1% BSA, pH 7.4) for 10 min at 37°C. Incubations were terminated by the addition of ice-cold perchloric acid [final concentration, 5% (v/v)]. Water-soluble inositol phosphates were then extracted with an equal volume of a 1:1 (v/v) mixture of 1,1,2-trichlorotrifluoroethane and tri-*N*-octylamine. The samples were mixed vigorously and centrifuged at 2500*g* for 30 min. The upper phase containing inositol phosphates was applied to an AG1-X8 resin column (Bio-Rad Laboratories, Hercules, CA). Inositol phosphates were eluted sequentially by the addition of an ammonium formate/formic acid solution of increasing ionic strength. Fractions containing inositol phosphates were collected and measured in a liquid scintillation counter.

Treatment with MTSEA. The MTSEA treatment was performed according to the procedure of Javitch et al. (1994), with minor modifications. Two days after transfection, the cells, which were grown in 12-well plates, were washed with PBS and incubated for 3 min at room temperature with freshly prepared MTSEA at the desired concentrations (typically from 0.5 to 6 mM) in a final volume of 0.2 ml. The reaction was stopped by washing the cells with ice-cold PBS. Intact cells were then incubated in binding medium (DMEM, 25 mM HEPES, pH 7.4, and 0.1% BSA) containing 0.05 nM ^{125}I-[Sar^1,Ile^8]AngII for 90 min at room temperature. After washing with ice-cold PBS, the cells were lysed with 0.1 N NaOH and radioactivity was evaluated by gamma counting. The percentage of fractional binding inhibition was calculated as [1 − (specific binding after MTSEA treatment/specific binding without treatment)] × 100.

Protection against MTSEA by [Sar^1,Ile^8]AngII. Transfected cells grown in 12-well plates were washed once with PBS and incubated in the presence or absence of 100 nM [Sar^1,Ile^8]AngII for 1 h at 16°C (to avoid internalization of receptors). The cells were washed to remove excess ligand and then treated with MTSEA. The cells were washed three times with ice-cold PBS and once with an acidic buffer (150 mM NaCl and 50 mM acetic acid, pH 3.0) to dissociate bound ligand. They were then incubated for 3 h at 16°C in binding medium (DMEM, 25 mM HEPES, pH 7.4, and 0.1% BSA) containing 0.05 nM ^{125}I-[Sar^1,Ile^8]AngII. The percentage of protection was calculated as [(inhibition in the absence of [Sar^1,Ile^8]AngII) − (inhibition in the

presence of [Sar[1],Ile[8]]AngII)/(inhibition in the absence of [Sar[1],Ile[8]]AngII)] × 100.

Data Analysis. Results are presented as means ± S.D. Binding data (B_{max} and K_d) were analyzed with Prism version 4.0 for Windows (GraphPad Software, San Diego CA), using a one-site binding hyperbola nonlinear regression analysis.

Results

Binding Properties of Mutant Receptors Bearing Cysteines in TMD6. To identify the residues in TMD6 that face the binding-site pocket of the AT_1 receptor, we mutated 26 consecutive residues between Lys240$^{(6.35)}$ and Leu265$^{(6.60)}$ to cysteine, one at a time (Fig. 1). Each mutant receptor was transiently expressed in COS-7 cells. To assess the conservation of the global conformation of these receptors after the substitutions, pharmacological parameters describing the equilibrium binding of the radiolabeled competitive ligand ^{125}I-[Sar[1],Ile[8]]AngII such as K_d and B_{max} were determined (Table 1 and Fig. 2). All mutant AT_1 receptors exhibited high binding affinity for ^{125}I-[Sar[1],Ile[8]]AngII (similar to that of the wild-type AT_1 receptor) except for mutants P255C$^{(6.50)}$ and D263C$^{(6.58)}$, which demonstrated no detectable binding activity and were not used for the SCAM analysis. B_{max} values for all detectable receptors ranged from 577 to 2630 fmol/mg.

Effect of Extracellularly Added MTSEA on the Binding Properties of Mutant Receptors. To verify whether the reporter cysteines introduced into TMD6 were oriented toward the binding pocket, mutant receptors were treated with concentrations of MTSEA varying between 0.5 and 6 mM. We had previously verified whether the wild-type AT_1 receptor, which contains 10 endogenous cysteines (Fig. 1), was sensitive to the MTSEA treatment and found that the various concentrations of MTSEA had very little effect (no more than a 25% reduction at high MTSEA concentrations) on the binding properties of the wild-type AT_1 receptor, indicating that the endogenous cysteines made a relatively small contribution to the binding-site pocket (Boucard et al., 2003).

When the AT_1 mutant receptors were treated with the alkylating agent, we found that a 3-min treatment with 2 mM MTSEA (Fig. 3) strongly inhibited the binding of F249C$^{(6.44)}$ (binding inhibition of 51%), H256C$^{(6.51)}$ (binding inhibition of 56%), T260C$^{(6.55)}$ (binding inhibition of 37%), and V264C$^{(6.59)}$ (binding inhibition of 67%). This binding inhibition was also observed at a lower concentration of MTSEA (0.5 mM). The mutant receptor A244C$^{(6.39)}$ was relatively insensitive to a treatment with 0.5 mM MTSEA, but its binding activity was slightly lower after a treatment with 2 mM MTSEA. The binding of all other mutant receptors was not significantly affected by MTSEA treatment. Overall, the most reactive cysteines were those substituted for Phe249$^{(6.44)}$, His256$^{(6.51)}$, Thr260$^{(6.55)}$, and Val264$^{(6.59)}$.

Altered Accessibility to TMD6 Reporter Cysteines in the Constitutively Active N111G-AT_1 Receptor. We made use of the constitutively active N111G-AT_1 receptor to assess and map the potentially altered accessibility of MTSEA to the engineered cysteines. We first determined the pharmacological properties of the 26 cysteine-substituted mutant receptors. Within the N111G-AT_1 receptor background, 24 cysteine-substituted mutants conserved a high binding affinity for the competitive ligand ^{125}I-[Sar[1],Ile[8]]AngII (Table 2 and Fig. 1), whereas one mutant (F249C$^{(6.44)}$-N111G-AT_1) displayed a moderate 4-fold decrease in binding affinity. The P255C$^{(6.50)}$-N111G-AT_1 receptor showed no detectable binding activity and was not used for the SCAM analysis. It is noteworthy, however, that the D263C$^{(6.58)}$ mutation, which exhibited a dramatic loss of binding in the wild-type receptor background, maintained its binding affinity when engineered in the N111G-AT_1 receptor background. B_{max} values for all detectable receptors ranged from 251 to 1350 fmol/mg (Table 2).

Figure 4 shows that, like the wild-type receptor, the N111G-AT_1 receptor was relatively insensitive to a 3-min treatment ranging from 0.5 to 2 mM MTSEA, again indicating the relatively low contribution of the endogenous cysteines in the binding-site pocket. Cysteine-substituted N111G-AT_1 receptor mutants were treated with increasing concentrations of MTSEA, and their binding properties were assessed with ^{125}I-[Sar[1],Ile[8]]AngII. Figure 4 summarizes the

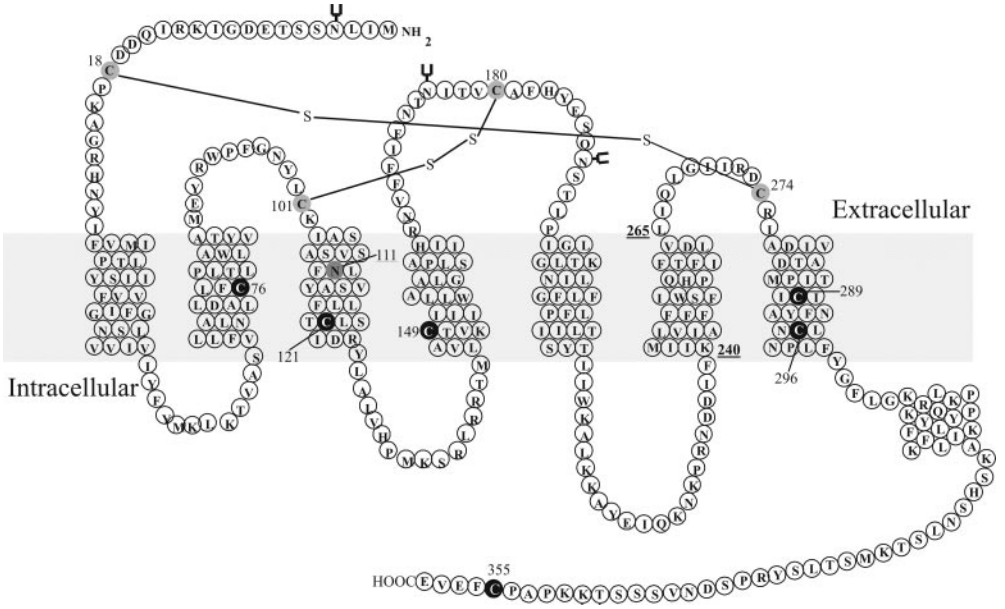

Fig. 1. Schematic representation of the human AT_1 receptor. The numbers indicate the positions of cysteines and other residues in the receptor. The gray circles represent cysteines that are thought to be linked via disulfide bridges, and the black circles represent cysteines whose side chains do not form a disulfide bridge. Mutated TMD6 residues are located between Lys[240] and Leu[265] inclusively. Asn-glycosylation sites (Asn[4], Asn[176], Asn[188]) are indicated. Asn[111] in TMD3 is also shown in gray.

effect of the MTSEA treatment on the cysteine-substituted N111G-AT_1 receptor mutants. As observed in the wild-type background, 0.5 mM MTSEA decreased the binding activity of the H256C$^{(6.51)}$-N111G-AT_1 mutant by 51%, the T260C$^{(6.55)}$-N111G-AT_1 mutant by 29%, and the V264C$^{(6.59)}$-N111G-AT_1 mutant by 23%. It is noteworthy that the W253C$^{(6.48)}$ and F261C$^{(6.56)}$ mutants, which were insensitive to MTSEA in the wild-type background, had reduced binding activity (32 and 27%, respectively) in the N111G-AT_1 background after a treatment with 2 mM MTSEA. On the other hand, F249C$^{(6.44)}$-N111G-AT_1, which exhibited a significant reduction in binding in the wild-type background, was insensitive to MTSEA in the N111G-AT_1 background. Finally, V264C$^{(6.59)}$-N111G-AT_1, which also exhibited a significant reduction in binding in the wild-type background (64%), had its binding inhibited by 23% when treated with 2 mM MTSEA.

Protection against MTSEA by a Pretreatment with [Sar^1,Ile^8]AngII. To confirm that reporter cysteines accessible to MTSEA were indeed located within the binding pocket, receptor mutants were incubated with the competitive ligand [Sar^1,Ile^8]AngII before MTSEA treatment. The cells were then washed with an acid buffer to dissociate the bound ligand, and the various receptors were assayed for binding with the radiolabeled competitive ligand. Figure 5 shows how a preincubation with the ligand protected mutant receptors F249C$^{(6.44)}$, H256C$^{(6.51)}$, T260C$^{(6.55)}$, V264C$^{(6.59)}$, N111G-H256C$^{(6.51)}$, and N111G-T260C$^{(6.55)}$ from the inhibitory effect of MTSEA, with protection levels ranging from 35% to 79%.

Functional Properties of Wild-Type, N111G, and MTSEA-Sensitive Mutant Receptors. The functional properties of wild-type, N111G, and mutant AT_1 receptors were evaluated by assessing the basal production of IPs in transiently transfected COS-7 cells. Figure 6 shows the relative amounts of IPs accumulated under basal conditions (white columns). The basal level of IPs found in cells expressing the cysteine mutant receptors in the wild-type background was as low as that found in cells expressing the wild-type receptor. The basal level of IPs found in cells expressing the cysteine mutants in the N111G background was higher than that found in cells expressing the wild-type AT_1 receptor, thereby demonstrating the constitutive activity of all receptors harboring both cysteine and N111G mutations. These results clearly show that cysteine mutations within TMD6 do not compromise the functional integrity of either the ground state AT_1 receptor or the constitutively active N111G-AT_1 receptor.

TABLE 1

Binding properties of cysteine-substituted mutant hAT_1 receptors

Cells transfected with the appropriate receptor were assayed as described under *Materials and Methods*. Binding affinities (K_d) and maximal binding capacities (B_{max}) are expressed as the means ± S.D. of values obtained in n independent experiments performed in duplicate. Mutants D263C and P255C demonstrated no detectable binding.

	K_d	B_{max}	n
	nM	*fmol/mg*	
WT	1.1 ± 0.4	1643 ± 1075	6
L265C	0.6 ± 0.2	1233 ± 457	3
V264C	0.8 ± 0.2	983 ± 329	3
L262C	1.1 ± 0.4	2630 ± 1151	3
F261C	1.0 ± 0.8	923 ± 587	3
T260C	1.1 ± 0.1	780 ± 79	3
F259C	0.8 ± 0.3	1553 ± 46	3
I258C	0.8 ± 0.2	2457 ± 284	3
Q257C	3.4 ± 1.3	903 ± 252	3
H256C	1.1 ± 0.2	1967 ± 72	3
I254C	0.7 ± 0.2	1657 ± 520	3
W253C	1.4 ± 0.3	1120 ± 825	3
S252C	1.0 ± 0.5	1217 ± 878	3
F251C	0.8 ± 0.5	1100 ± 377	3
F250C	1.0 ± 0.3	1317 ± 488	3
F249C	1.6 ± 0.3	837 ± 205	3
F248C	1.0 ± 0.3	767 ± 238	3
L247C	0.8 ± 0.2	620 ± 365	3
V246C	0.9 ± 0.1	577 ± 248	3
I245C	0.9 ± 0.2	1503 ± 540	3
A244C	0.6 ± 0.2	790 ± 516	3
M243C	0.7 ± 0.2	1200 ± 576	3
I242C	0.5 ± 0.1	1293 ± 539	3
I241C	0.7 ± 0.2	1240 ± 519	3
K240C	0.7 ± 0.1	1440 ± 357	3

Discussion

The rationale of this study, which relied on SCAM analysis, was to gain an insight into the orientation of TMD6 of the AT_1 receptor by identifying the residues accessible to MTSEA within the binding site pocket. Mapping these residues in the ground state receptor and the constitutively active N111G background allowed us to measure relative changes in the position of certain residues, thus providing valuable information with which to infer a structural change underlying AT_1 receptor activation. It is important to mention that the [Sar^1,Ile^8]AngII used in our study is an antagonist on the wild-type AT_1 receptor. We (Clément et al., 2006) and others

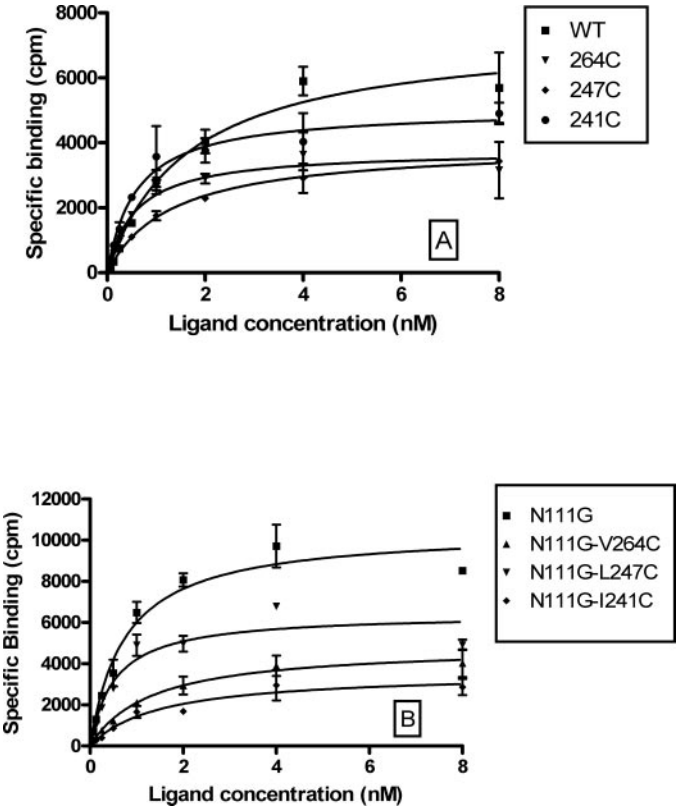

Fig. 2. Binding properties of AT_1 cys-mutant and AT_1-N111G cys-mutant receptors. Mutant receptors were expressed in COS-7 cells, and their binding properties were determined by saturation binding experiments as indicated under *Materials and Methods*. The results are representative of three independent experiments, the mean ± S.D. values of which are reported in Tables 1 and 2.

(Le et al., 2003; Ellis et al., 2006) have demonstrated that [Sar^1,Ile^8]AngII is a full agonist on the constitutively active N111G AT_1 receptor. Thus, [Sar^1,Ile^8]AngII does not act as inverse agonist (as do many antagonists on their cognate receptor) on the N111G AT_1 receptor but would rather act to maintain the receptor in its active state, thereby justifying its use herein.

As reported previously, the insensitivity of the wild-type receptor to MTSEA suggests either that endogenous cysteines are not alkylated by MTSEA or that their alkylation does not affect the binding of the ligand (Boucard et al., 2003). Our approach of adding the MTSEA reagent to whole adherent cells expressing the AT_1 receptor essentially exposed only the extracellular ligand-accessible side of the receptor to MTSEA. The robustly sensitive residues that we identified with the SCAM approach lie in the middle [H256C$^{(6.51)}$, T260C$^{(6.55)}$] to top portion of TMD6 (V264C$^{(6.59)}$) (Fig. 2). In addition, TMD6 possesses one robustly sensitive residue [Phe249$^{(6.44)}$] that is located in the middle of the TMD but more proximal to the cytoplasmic side.

The sensitivity of residue Val264$^{(6.59)}$ to MTSEA would delineate the top of the binding pocket, whereas residue Phe249$^{(6.44)}$ would delineate the bottom of the water-accessible binding pocket of the AT_1 receptor. Along with these residues, two other residues, His256$^{(6.51)}$ and Thr260$^{(6.55)}$, would lie on the same α-helix face in the ground state of the receptor, with appreciable exposure to a potential hydrophilic pocket. Alkylation with MTSEA would hamper the binding of the ligand in a mechanism involving steric hindrance, electrostatic repulsion, or indirect interaction. Furthermore, it is assumed that water-accessible residues are located in the binding site pocket if a competitive ligand protects them from the effect of MTSEA. The competitive ligand [Sar^1,Ile^8]AngII protected all the residues tested in the protection assay, thus supporting the notion that these specific residues within TMD6 are located in the binding pocket. Although the A244C$^{(6.39)}$ mutant did show sensitivity, we did not consider this residue to be in the binding pocket because 1) it was at the limit of detectability only at 2 mM MTSEA in our assay conditions and 2) it is not on the same helical face as the other positive residues discussed above.

Our finding that these residues were located in the binding pocket of the AT_1 receptor is in accordance with the current models proposed for bovine rhodopsin (Palczewski et al., 2000) and the dopamine D2 receptor (Javitch et al., 1998) and with our recent methionine proximity assay (MPA) study of the AT_1 receptor (Clément et al., 2005). Indeed, residues Phe261$^{(6.44)}$, Trp265$^{(6.48)}$, and Tyr268$^{(6.51)}$ are thought to be contact points with retinal in the crystal structure of bovine rhodopsin (Palczewski et al., 2000), whereas the SCAM approach was used to show that residues Phe382$^{(6.44)}$, Trp386$^{(6.48)}$, Phe389$^{(6.51)}$, His393$^{(6.55)}$, and Ile397$^{(6.59)}$ are located in the binding pocket of dopamine D2 receptor (Javitch et al., 1998). Moreover, using another approach (MPA), we identified several residues in TMD6 [positions Phe249$^{(6.44)}$, Trp253$^{(6.48)}$, His256$^{(6.51)}$, and Thr260$^{(6.55)}$] that react with the carboxyl terminus of the photoreactive ligand. These studies showed that position 6.48, a well conserved trypto-

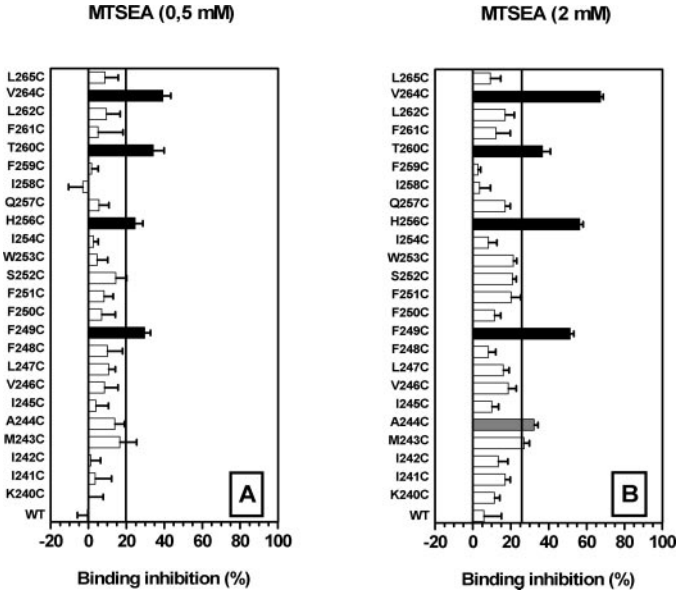

Fig. 3. Effects of MTSEA on AT_1 receptor mutants bearing a reporter cysteine in TMD6. Intact COS-7 cells transiently expressing wild-type or mutant AT_1 receptors were incubated for 3 min at room temperature with freshly prepared 0.5 mM MTSEA (A) or 2 mM MTSEA (B). The intact cells were then incubated for 90 min at room temperature with 0.05 nM ^{125}I-[Sar^1,Ile^8]AngII. The percentage of binding inhibition was calculated as indicated under *Materials and Methods*. The vertical line represents an arbitrary threshold used to identify cysteine-sensitive mutants and was set at a value corresponding to binding inhibition 20% greater than that of the wild-type AT_1 receptor. The white bars indicate mutant receptors for which binding activities were not appreciably reduced compared with the wild-type receptor after treatment with MTSEA. The black bars indicate mutant receptors for which binding activities were reduced after treatment with MTSEA. The gray bar represents a mutant that exhibited an odd sensitivity to MTSEA. Each bar represents the mean ± S.D. of data from at least three independent experiments.

TABLE 2

Binding properties of cysteine-substituted mutant hAT_1 receptors bearing the Asn^{111}Gly mutation

Cells transfected with the appropriate receptor were assayed as described under *Materials and Methods*. Binding affinities (K_d) and maximal binding capacities (B_{max}) are expressed as the means ± S.D. of values obtained in n independent experiments performed in duplicate. Mutant N111G-P255C demonstrated no detectable binding.

	K_d	B_{max}	n
	nM	*fmol/mg*	
N111G	1.0 ± 0.4	1100 ± 682	4
L265C	0.8 ± 0.5	389 ± 417	3
V264C	1.9 ± 0.7	1179 ± 791	3
D263C	0.9 ± 0.3	251 ± 197	3
L262C	1.1 ± 0.1	735 ± 522	3
F261C	1.0 ± 0.3	894 ± 385	3
T260C	1.7 ± 0.7	1265 ± 918	3
F259C	0.4 ± 0.1	805 ± 983	3
I258C	0.7 ± 0.1	489 ± 460	3
Q257C	2.3 ± 1.3	451 ± 404	3
H256C	1.0 ± 0.3	574 ± 400	3
I254C	0.4 ± 0.1	688 ± 438	3
W253C	0.8 ± 0.1	588 ± 376	3
S252C	0.6 ± 0.2	1175 ± 1098	3
F251C	0.9 ± 0.5	704 ± 499	3
F250C	1.8 ± 0.6	661 ± 375	4
F249C	3.9 ± 1.2	744 ± 517	4
F248C	0.3 ± 0.0	1513 ± 892	3
L247C	0.7 ± 0.2	968 ± 502	3
V246C	0.7 ± 0.1	1001 ± 571	3
I245C	1.3 ± 0.2	1076 ± 256	3
A244C	1.2 ± 0.3	1201 ± 893	3
M243C	1.0 ± 0.2	1346 ± 638	3
I242C	1.0 ± 0.1	1161 ± 306	3
I241C	1.1 ± 0.6	951 ± 371	3
K240C	1.1 ± 0.3	1122 ± 653	3

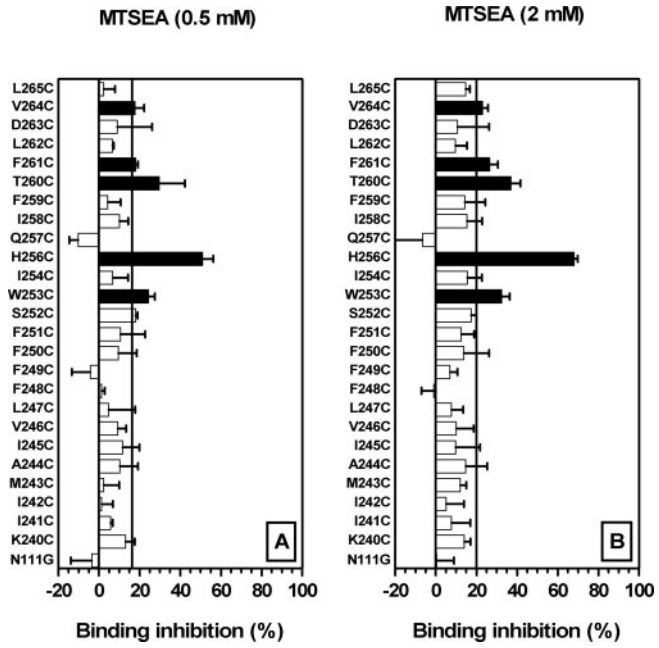

Fig. 4. Effect of MTSEA on N111G-AT_1 receptor mutants bearing a reporter cysteine in TMD6. Intact COS-7 cells transiently expressing the mutant N111G-AT_1 receptors were incubated for 3 min at room temperature with freshly prepared 0.5 mM MTSEA (A) or 2 mM MTSEA (B). The intact cells were then incubated for 90 min at room temperature with 0.05 nM ^{125}I-[Sar^1,Ile^8]AngII. The percentage of binding inhibition was calculated as indicated under *Materials and Methods*. The vertical line represents an arbitrary threshold used to identify cysteine-sensitive mutants. It was set at a value corresponding to binding inhibition 20% greater than that of the N111G-AT_1 receptor. The white bars indicate mutant receptors for which binding activities were not appreciably reduced compared with that of the N111G-AT_1 receptor after treatment with MTSEA. The black bars indicate mutant receptors for which binding activities were reduced after treatment with MTSEA. Each bar represents the mean ± S.D. of data from at least three independent experiments.

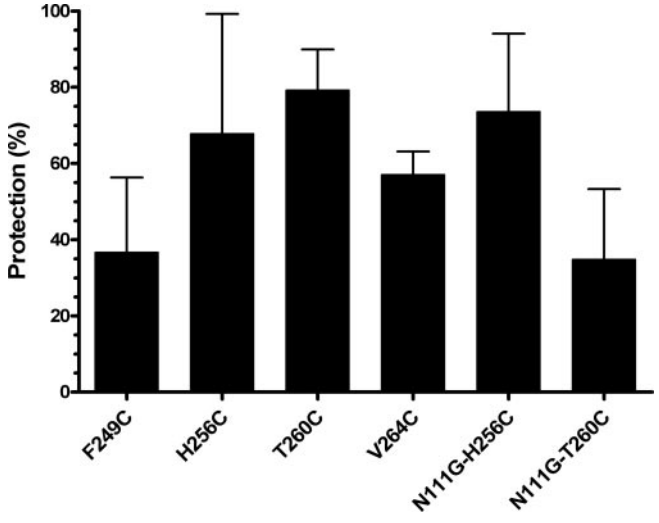

Fig. 5. [Sar^1,Ile^8]AngII protection of MTSEA-sensitive receptor mutants. Intact COS-7 cells transiently expressing the indicated MTSEA-sensitive mutant AT_1 receptors were preincubated for 1 h at 16°C in the absence or presence of 100 nM [Sar^1,Ile^8]AngII. The cells were then incubated for 3 min at 16°C in the continued absence or presence of [Sar^1,Ile^8]AngII with optimal MTSEA concentrations to achieve maximal binding inhibition of each receptor. The MTSEA concentrations were as follows: 0.5 mM for F249C-AT_1, H256C-AT_1, T260C-AT_1, V264C-AT_1, H256C-N111G-AT_1, and T260C-N111G-AT_1. The cells were then washed with ice-cold PBS and incubated for 3 h at 16°C with 0.05 nM ^{125}I-[Sar^1,Ile^8]AngII. Protection was calculated as described under *Materials and Methods*. Each bar represents the mean ± S.D. of data from at least three independent experiments.

phan residue found in many (40%; see Table 3) class A receptors, is located in the binding pocket. The present SCAM study identified Trp253$^{(6.48)}$ in the N111G-AT_1 receptor background but not in the ground state, which may be explained by the toggle switch mechanism (see below). In light of these results, the orientation of conserved positions within the ligand-binding pocket may be a common feature of TMD6 of class A GPCRs.

To further investigate the mechanism by which the AT_1

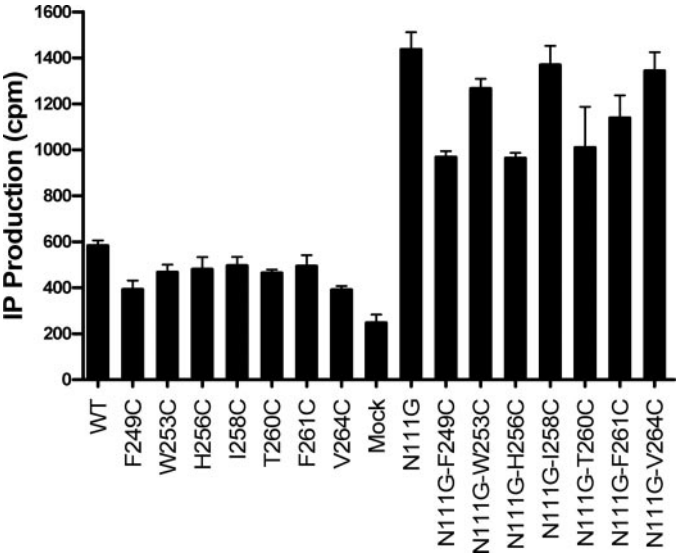

Fig. 6. Basal level of IPs in cells expressing the wild type and mutant AT_1 receptors. Transfected COS-7 cells were loaded for 16 to 24 h with 10 μCi/ml [*myo*-^{3}H]-inositol in inositol-free M199 medium. IP levels (sum of inositol bisphosphate, inositol trisphosphate, and inositol tetrakisphosphate) were determined as described under *Materials and Methods*. These results represent the means ± SDs of one experiment (done in triplicate with comparable results) where IP production was normalized.

TABLE 3

Homology of the TMD6 AT_1 side chain among rhodopsin-like GPCRs

The frequency of the side chains in this TMD was compared with all receptors in the rhodopsin family (class A) obtained from the GPCRDB information system (http://www.gpcr.org/7tm/).

AT_1 Residue	Frequency of Occurrence	Conserved Residue	Frequency of Occurrence
	%		%
Leu265 (6.60)	16.7		
Val264 (6.59)	11.0		
Asp263 (6.58)	7.2		
Leu262 (6.57)	22.3		
Phe261 (6.56)	10.1		
Thr260 (6.55)	4.1		
Phe259 (6.54)	13.1		
Ile258 (6.53)	16.1		
Gln257 (6.52)	5.4	Phe or His	25.6
His256 (6.51)	2.9	Phe or Tyr	43.1
Pro255 (6.50)	76.7		
Ile254 (6.49)	9.0		
Trp253 (6.48)	40.2		
Ser252 (6.47)	8.7	Cys	36.8
Phe251 (6.46)	5.5	Leu, Ile, or Ser	48.6
Phe250 (6.45)	14.1		
Phe249 (6.44)	42.7		
Phe248 (6.43)	3.6	Thr, Ala, Val, Leu, or Ile	68.5
Leu247 (6.42)	12.3		
Val246 (6.41)	28.9		
Ile245 (6.40)	13.1		
Ala244 (6.39)	11.0		

receptor undergoes structural changes during the transition from its inactive to its active state, we took advantage of the constitutively active N111G-AT_1 receptor. It is believed that the isomerization of conformers toward the active state, which involves TMD movement, is stabilized by the binding of an agonist, and may be mimicked in part by the constitutively active receptor (Gether and Kobilka, 1998; Seifert and Wenzel-Seifert, 2002). We thus verified the accessibility of TMD6 residues to MTSEA within the structural background of the N111G-AT_1 receptor. We compared the pattern obtained with that of the wild-type receptor and found that the Cys-substituted residues $His256^{(6.51)}$ and $Thr260^{(6.55)}$ maintained their sensitivity to MTSEA. Two additional Cys-substituted residues [$Trp253^{(6.48)}$ and $Phe261^{(6.56)}$] were found to be sensitive to MTSEA. It is noteworthy that, in the N111G-AT_1 background, the sensitivity of $Phe249^{(6.44)}$ to MTSEA was completely abolished and the sensitivity of $Val264^{(6.59)}$ was greatly diminished compared with the basal state. Thus, in the active state of the receptor, $Phe249^{(6.44)}$, which is located more toward the bottom of the TMD, would be displaced from the binding pocket. In the protection assay for the N111G-AT_1 receptor background, the competitive ligand [Sar^1,Ile^8]AngII offered effective protection to the sensitive mutants [$His256^{(6.51)}$ and $Thr260^{(6.55)}$] against the alkylating effect of MTSEA, suggesting that these residues are located in the binding pocket.

The divergence in the sensitive Cys-substituted residues between the wild-type AT_1 receptor and the N111G-AT_1 receptor (Fig. 7) suggests that the accessibility of residues in TMD6 and their spatial proximity within the binding pocket were altered as a result of the single substitution of Asn111 for Gly in TMD3. Our results point to a significant structural change during the process of activation of the receptor. Because $His256^{(6.51)}$ and $Thr260^{(6.55)}$, which are located in the middle of the TMD, were still MTSEA-sensitive in the N111G background, we may have expected that Trp253, which is located on the same helical face, would become MTSEA-sensitive in the constitutive receptor background, as discussed above. Using MPA, we had previously identified $Trp253^{(6.48)}$ in the binding pocket of the basal state of the receptor (Clément et al., 2005). Here, the gain in sensitivity to MTSEA of $Trp253^{(6.48)}$ could be explained by the rotamer toggle switch mechanism previously reported for rhodopsin (Lin and Sakmar, 1996; Schwartz et al., 2006; Smit et al., 2007) and the β2-adrenergic receptor (Shi et al., 2002). In rhodopsin, this conserved residue, which is found in numerous class A GPCRs, undergoes a conformational transition when the receptor goes from the ground state to the active state. This is due to a disruption of hydrogen bond networks formed through $Asp^{(2.50)}$, $Asn^{(7.45)}$, and water molecules, which shifts the orientation of $Trp253^{(6.48)}$ from pointing toward TMD7 to pointing toward TMD5 upon receptor activation (Ruprecht et al., 2004). Thus, the nonreactivity of W253C in the basal state could be due to similar intramolecular interactions of the introduced cysteine with residues of other TMDs, rendering it inaccessible to MTSEA, whereas in the N111G constitutively active receptor background, reorientation of the side chain of this residue would make it more susceptible to alkylation by MTSEA.

We therefore propose that the middle portion of TMD6 does not move extensively during the activation of the AT_1 receptor. In the N111G-mutant background, $F261C^{(6.56)}$, which is near the top of TMD6, became MTSEA-sensitive. This residue is located at the periphery of the helical face formed by

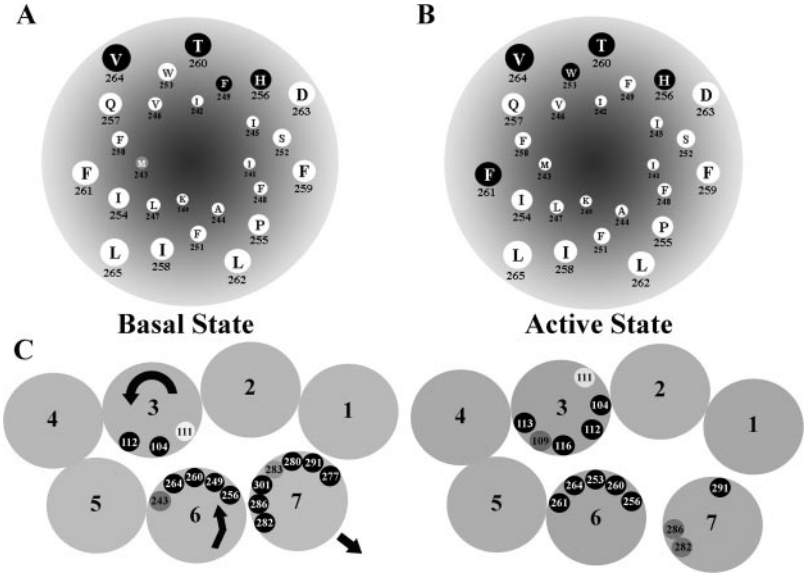

Fig. 7. A and B, helical wheel representation of TMD6 reporter cysteines and their pattern of reactivity to MTSEA. Positions in TMD6 of MTSEA-alkylated cysteines affecting ligand binding are shown in a helical wheel representation viewed from the extracellular side (A) for receptors with no additional mutation in TMD3 and (B) for receptors in which $Asn111^{(3.35)}$ had been mutated to Gly in addition to the reporter cysteine in TMD3. The gray and black circles indicate mutant receptors for which binding activities were slightly reduced (gray) or significantly reduced (black) after the treatment with MTSEA. White circles indicate those mutant receptors that had no effect on ligand binding when reacted with MTSEA or positions that resulted in little or no detectable binding when substituted for cysteines. C, proposed structurally related activation mechanisms for AT_1 receptor. Positions of TMDs as viewed from the extracellular side, based on the model described for bovine rhodopsin (Palczewski et al., 2000). Residues that were sensitive to MTSEA treatment in TMDs 3, 6, and 7 are indicated. The dark gray and black circles indicate mutant receptors for which binding activities were slightly reduced (gray) or significantly reduced (black) after treatment with MTSEA. Asn^{111} in TMD3 is shown in light gray. Arrows depict the proposed movements of each TMD during the activation process. In the present study, we suggest that TMD6 undergoes a pivot movement, bringing the top of the TMD closer to the binding crevice while the bottom part would move away from the binding crevice.

the MTSEA-sensitive V264C$^{(6.59)}$, T260C$^{(6.55)}$, H256C$^{(6.51)}$, and F249C$^{(6.44)}$ residues identified in the ground state (see Fig. 7). Such a gain in sensitivity may signify that, upon activation, the top of TMD6 may rotate clockwise, thereby enabling F261C$^{(6.56)}$ to enter the binding pocket and be alkylated. The significant reduction of sensitivity of V264C$^{(6.59)}$ to MTSEA in the N111G constitutively active receptor background compared with the wild-type basal state also suggests that, although it remains in the binding pocket, both the position/orientation of V264C$^{(6.59)}$ and the top of TMD6 change in the activation process.

For residues located deeper in TMD6, we observed that Phe249$^{(6.44)}$ was highly sensitive in the ground state and became nonsensitive in the N111G background. One possibility is that along with the rotation of the top of TMD6, the bottom of the helix may independently undergo a pivoting action away from the lower part of the pocket. Another simpler alternative to explain our results could be that, during the process of AT_1 receptor activation, TMD6 undergoes integral pivoting (without additional movements in the top or bottom of the TMD), bringing the top of the TMD toward the binding pocket and pushing the bottom away from the binding pocket. This straightforward pivoting movement would expose Phe261$^{(6.56)}$ to the binding pocket and extrude Phe249$^{(6.44)}$ out of the binding pocket (Fig. 8). This explanation would go along with the four proposed simple but varied types of movements (pivoting, rotation, translation, piston movement) that TMD α-helices can undergo in a lipid bilayer (Matthews et al., 2006).

In conclusion, our data comparing the ground state to the activated state of the AT_1 receptor point toward a pivoting movement of TMD6 that exposes Phe261$^{(6.56)}$ and alters the exposure of Val264$^{(6.59)}$ to a water-accessible crevice. The outward movement of the bottom of TMD6 would shift Phe249$^{(6.44)}$ away from the binding pocket. This movement would contribute to the structural relaxation of the activated receptor and would facilitate the flexibility of the third cytoplasmic loop, enabling binding and/or activation of the cognate G protein as recently suggested for rhodopsin (Salom et al., 2006). The pivoting movement of TMD6 upon activation of the AT_1 receptor is reminiscent of the inward movement of the extracellular segment and outward movement of the intracellular segment of TMD6 recently observed with the β_2-adrenergic receptor (Elling et al., 2006). This particular movement may thus be a structural feature common to numerous rhodopsin-like GPCRs.

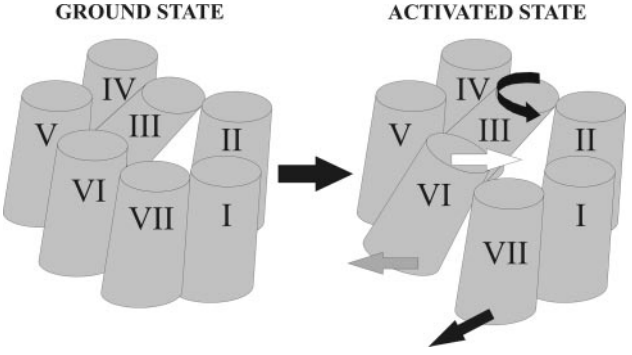

Fig. 8. Proposed structurally related activation mechanisms for the AT_1 receptor. An extracellular view of the seven TMDs of the AT_1 receptor based on the model described for bovine rhodopsin (Palczewski et al., 2000). The water-accessible crevice forming the binding pocket is suggested to be located between TMDs 1, 2, 3, 5, 6, and 7. In the ground state, constraining intramolecular interactions help maintain the receptor in a basal state where functional coupling with the G-protein is kept to a minimum. During the process of activation (after agonist binding), intramolecular interactions are broken and the receptor goes through a series of conformational rearrangements involving the different TMDs. We recently provided data suggesting that TMD7 can be excluded from the water-filled binding crevice by a translational movement (Boucard et al., 2003) and that TMD3 rotates slightly on its axis during activation of the AT_1 receptor (Martin et al., 2004). In addition, we now suggest a pivoting movement of TMD6. Such a movement of the intracellular segment of TMD6 is functionally coupled to an opposite movement of the extracellular segment of TMD6 (i.e., toward the ligand-binding pocket). The white arrows indicate the inward movement of the extracellular segments of TMD6, and the gray arrows indicate the outward movement of the intracellular segments of the helices.

References

Akabas MH, Stauffer DA, Xu M, and Karlin A (1992) Acetylcholine receptor channel structure probed in cysteine-substitution mutants. *Science* **258:**307–310.

Ballesteros JA and Weinstein H (1995) *Integrated Methods for the Construction of Three-Dimensional Models and Computational Probing of Structure-Function Relations in G Protein-Coupled Receptors.* Academic Press, San Diego, CA.

Balmforth AJ, Lee AJ, Warburton P, Donnelly D, and Ball SG (1997) The conformational change responsible for AT1 receptor activation is dependent upon two juxtaposed asparagine residues on transmembrane helices III and VII. *J Biol Chem* **272:**4245–4251.

Boucard AA, Roy M, Beaulieu ME, Lavigne P, Escher E, Guillemette G, and Leduc R (2003) Constitutive activation of the angiotensin II type 1 receptor alters the spatial proximity of transmembrane 7 to the ligand-binding pocket. *J Biol Chem* **278:**36628–36636.

Burnier M (2001) Angiotensin II type 1 receptor blockers. *Circulation* **103:**904–912.

Clément M, Chamberland C, Perodin J, Leduc R, Guillemette G, and Escher E (2006) The active and the inactive form of the hAT1 receptor have an identical ligand-binding environment: an MPA study on a constitutively active angiotensin II receptor mutant. *J Recept Signal Transduct Res* **26:**417–433.

Clément M, Martin SS, Beaulieu ME, Chamberland C, Lavigne P, Leduc R, Guillemette G, and Escher E (2005) Determining the environment of the ligand binding pocket of the human angiotensin II type I (hAT1) receptor using the methionine proximity assay. *J Biol Chem* **280:**27121–27129.

Corpet F (1988) Multiple sequence alignment with hierarchical clustering. *Nucleic Acids Res* **16:**10881–10890.

de Gasparo M, Catt KJ, Inagami T, Wright JW, and Unger T (2000) International union of pharmacology. XXIII. The angiotensin II receptors. *Pharmacol Rev* **52:**415–472.

Dunham TD and Farrens DL (1999) Conformational changes in rhodopsin. Movement of helix f detected by site-specific chemical labeling and fluorescence spectroscopy. *J Biol Chem* **274:**1683–1690.

Elling CE, Frimurer TM, Gerlach LO, Jorgensen R, Holst B, and Schwartz TW (2006) Metal ion site engineering indicates a global toggle switch model for seven-transmembrane receptor activation. *J Biol Chem* **281:**17337–17346.

Ellis J, Warburton P, Donnelly D, and Balmforth AJ (2006) Conformational induction is the key process for activation of the AT1 receptor. *Biochem Pharmacol* **71:**464–471.

Feng YH, Miura S, Husain A, and Karnik SS (1998) Mechanism of constitutive activation of the AT1 receptor: influence of the size of the agonist switch binding residue Asn(111). *Biochemistry* **37:**15791–15798.

Fraker PJ and Speck JC, Jr (1978) Protein and cell membrane iodinations with a sparingly soluble chloroamide,1,3,4,6-tetrachloro-3a,6a-diphrenylglycoluril. *Biochem Biophys Res Commun* **80:**849–857.

Gether U and Kobilka BK (1998) G protein-coupled receptors. II. Mechanism of agonist activation. *J Biol Chem* **273:**17979–17982.

Ghanouni P, Steenhuis JJ, Farrens DL, and Kobilka BK (2001) Agonist-induced conformational changes in the G-protein-coupling domain of the beta 2 adrenergic receptor. *Proc Natl Acad Sci U S A* **98:**5997–6002.

Groblewski T, Maigret B, Larguier R, Lombard C, Bonnafous JC, and Marie J (1997) Mutation of Asn111 in the third transmembrane domain of the AT1A angiotensin II receptor induces its constitutive activation. *J Biol Chem* **272:**1822–1826.

Guillemette G and Escher E (1983) Analysis of the adrenal angiotensin II receptor with the photoaffinity labeling method. *Biochemistry* **22:**5591–5596.

Inoue Y, Nakamura N, and Inagami T (1997) A review of mutagenesis studies of angiotensin II type 1 receptor, the three-dimensional receptor model in search of the agonist and antagonist binding site and the hypothesis of a receptor activation mechanism. *J Hypertens* **15:**703–714.

Javitch JA, Ballesteros JA, Weinstein H, and Chen J (1998) A cluster of aromatic residues in the sixth membrane-spanning segment of the dopamine D2 receptor is accessible in the binding-site crevice. *Biochemistry* **37:**998–1006.

Javitch JA, Li X, Kaback J, and Karlin A (1994) A cysteine residue in the third membrane-spanning segment of the human D2 dopamine receptor is exposed in the binding-site crevice. *Proc Natl Acad Sci U S A* **91:**10355–10359.

Javitch JA, Shi L, and Liapakis G (2002) Use of the substituted cysteine accessibility method to study the structure and function of G protein-coupled receptors. *Methods Enzymol* **343:**137–156.

Lanctot PM, Leclerc PC, Escher E, Leduc R, and Guillemette G (1999) Role of *N*-glycosylation in the expression and functional properties of human AT1 receptor. *Biochemistry* **38:**8621–8627.

Le MT, Vanderheyden PM, Szaszak M, Hunyady L, Kersemans V, and Vauquelin G (2003) Peptide and nonpeptide antagonist interaction with constitutively active human AT1 receptors. *Biochem Pharmacol* **65:**1329–1338.
Lin SW and Sakmar TP (1996) Specific tryptophan UV-absorbance changes are probes of the transition of rhodopsin to its active state. *Biochemistry* **35:**11149–11159.
Martin SS, Boucard AA, Clément M, Escher E, Leduc R, and Guillemette G (2004) Analysis of the third transmembrane domain of the human type 1 angiotensin II receptor by cysteine scanning mutagenesis. *J Biol Chem* **279:**51415–51423.
Matthews EE, Zoonens M, and Engelman DM (2006) Dynamic helix interactions in transmembrane signaling. *Cell* **127:**447–450.
Miura S, Saku K, and Karnik SS (2003) Molecular analysis of the structure and function of the angiotensin II type 1 receptor. *Hypertens Res* **26:**937–943.
Palczewski K, Kumasaka T, Hori T, Behnke CA, Motoshima H, Fox BA, Le Trong I, Teller DC, Okada T, Stenkamp RE, et al. (2000) Crystal structure of rhodopsin: A G protein-coupled receptor. *Science* **289:**739–745.
Rasmussen SG, Jensen AD, Liapakis G, Ghanouni P, Javitch JA, and Gether U (1999) Mutation of a highly conserved aspartic acid in the beta2 adrenergic receptor: constitutive activation, structural instability, and conformational rearrangement of transmembrane segment 6. *Mol Pharmacol* **56:**175–184.
Ruprecht JJ, Mielke T, Vogel R, Villa C, and Schertler GF (2004) Electron crystallography reveals the structure of metarhodopsin I. *EMBO J* **23:**3609–3620.
Salom D, Lodowski DT, Stenkamp RE, Trong IL, Golczak M, Jastrzebska B, Harris T, Ballesteros JA, and Palczewski K (2006) Crystal structure of a photoactivated deprotonated intermediate of rhodopsin. *Proc Natl Acad Sci U S A* **103**:16123–16128.
Schwartz TW, Frimurer TM, Holst B, Rosenkilde MM, and Elling CE (2006) Molecular mechanism of 7TM receptor activation–a global toggle switch model. *Annu Rev Pharmacol Toxicol* **46:**481–519.
Seifert R and Wenzel-Seifert K (2002) Constitutive activity of G-protein-coupled receptors: cause of disease and common property of wild-type receptors. *Naunyn Schmiedebergs Arch Pharmacol* **366:**381–416.
Shi L, Liapakis G, Xu R, Guarnieri F, Ballesteros JA, and Javitch JA (2002) β2 adrenergic receptor activation. Modulation of the proline kink in transmembrane 6 by a rotamer toggle switch. *J Biol Chem* **277:**40989–40996.
Smit MJ, Vischer HF, Bakker RA, Jongejan A, Timmerman H, Pardo L, and Leurs R (2007) Pharmacogenomic and structural analysis of constitutive G protein-coupled receptor activity. *Annu Rev Pharmacol Toxicol* **47:**53–87.

Address correspondence to: Richard Leduc, Department of Pharmacology, Faculty of Medicine and Health Sciences, Université de Sherbrooke, 3001 12th Avenue North, Sherbrooke, Quebec, Canada, J1H 5N4.E-mail: richard.leduc@usherbrooke.ca